JCTC Journal of Chemical Theory and Computation

Article

pubs.acs.org/JCTC

# Conformational Effects on the Magnetic Properties of an Organic Diradical: A Computational Study

Vincenzo Barone,*[,†] Corentin Boilleau,[†] Ivo Cacelli,[‡] Alessandro Ferretti,[§] and Giacomo Prampolini[∥]

[†]Scuola Normale Superiore, Piazza dei Cavalieri, I-56126 Pisa, Italy

[‡]Dipartimento di Chimica e Chimica Industriale, Università di Pisa, Via Risorgimento 35, 56126 Pisa, Italy

[§]Istituto di Chimica dei Composti OrganoMetallici del CNR, Area della Ricerca di Pisa, Via G. Moruzzi 1, I-56122 Pisa, Italy

[∥]Istituto per i Processi Chimico-Fisici (IPCF-CNR), Area della Ricerca, via G. Moruzzi 1, I-56124 Pisa, Italy

**ABSTRACT:** A theoretical study on the singlet triplet energy splitting in a *m*-phenylene bridged organic diradical has been performed using an original computational protocol developed in our group. The method is based on post Hatree−Fock calculations and has proven to provide accurate results with reasonable computational effort. By virtue of such efficiency, the full PES of both the singlet and triplet states as a function of the two "soft" torsional degrees of freedom at the meta position of the ring has been explored. In agreement with literature findings, we found a pronounced dependence of the sign of the energy gap from the torsional angles. Finally, exploiting the two-dimensional surface, a statistical analysis is carried out at low temperatures and a comparison with available experimental data addressed.

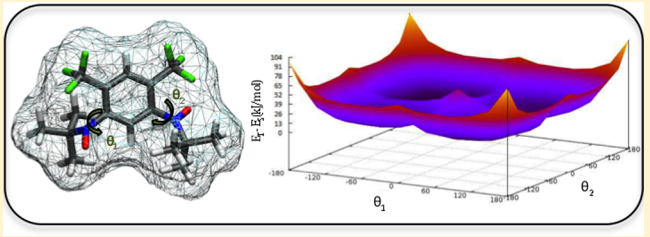


## INTRODUCTION

Owing to both their theoretical and technological interest, open shell organic diradicals have been studied for a long time.[1−4] Their peculiar properties stem from the interaction of unpaired electrons localized in separate fragments of the same molecule, which usually communicate through aromatic moieties connecting them, hence indicated as "bridges." This characteristic might be exploited to operate, by means of external actions, molecular changes able to tune the intensity of the exchange interaction, or even to switch between ferromagnetic and antiferromagnetic behavior. Specific diradicals can be designed so to be assembled in the construction of polyradical systems with potential application as organic-based memories.[5−8] From this perspective, organic diradicals based on phenylene bridges seem to be very good and promising candidates.[1,9]

All molecular-based magnets, being either organic or inorganic, share the common problem that an accurate prediction of their properties at the microscopic level is a very hard task, especially for large systems. On the other hand, the understanding of the spin−spin interactions underlying the observed magnetic properties of the molecule is the key for governing them and may then also aid in the design of new functional species.

From the theoretical and computational point of view, we are then called to develop computational recipes able to give reliable values of the energy gap between the several electronic states with different spins, possibly suitable for large sized molecules,

As far as diradicals are concerned, we need to calculate the energy gap between the triplet and the singlet states, which in terms of the Heisenberg−Dirac−Van Vleck model corresponds to the spin−spin coupling term $\Delta E = E_S - E_T = J$. This quantity may be easily obtained in the Density Functional Theory (DFT) framework through the Noodleman broken-symmetry method,[10,11] in order to overcome the problem of the multideterminantal nature of the singlet ground state. However, accurate and reliable values of $J$ can only be pursued in more solid post Hartree−Fock approaches.[12−28] In order to obtain reliable results, variational calculations are to be preferred in comparison to perturbative approaches, because in the latter the neglect of the interaction terms between the perturbers could invalidate the accuracy of the results.[22] This can be a computational bottleneck for large systems, where the dimension of the CI space is seen rapidly to grow. From this perspective, Difference Dedicated Configuration Interaction (DDCI),[13,14] where the CI space is chosen according to the contribution of the various classes of excitations, represents the first attempt to balance accuracy and computational cost. Indeed, DDCI-based calculations are now currently performed for metallic and organic magnetic species. In order to improve the performance of DDCI, one can complement the method using fragmentation techniques[23,24] and modified virtual orbitals[29] and tuning a balanced variational-perturbative calculation where the accurate variational values of the energy of the singlet and triplet states are refined by means of Möller−Plesset second order perturbation corrections.[30,31]

The method has been recently validated for the para and meta phenyl-bridged nitroxides model species (HNO−phenyl−

**Received:** January 8, 2013
**Published:** February 21, 2013

   dx.doi.org/10.1021/ct400020x | *J. Chem. Theory Comput.* 2013, 9, 1958−1963

ONH), characterized by antiferromagnetic (para-isomer) and ferromagnetic (meta-isomer) character.[32] Successive applications to other 1,3-phenylene-bridged molecular systems[30,31] have further clarified the validity of such an approach, which has now been implemented in a new, modern, and efficient code for multireference configuration interaction calculations, named BALOO, which will be presented elsewhere.

Here, BALOO has been applied to the extensive calculation of the singlet−triplet energy gap in 4,6-trifluoromethyl *m*-phenylene bis(tert-butyl)-nitroxide (NOFB; Figure 1) in the two-dimensional space of the two torsional angles driving the internal rotation of the *tert*-butyl moiety.

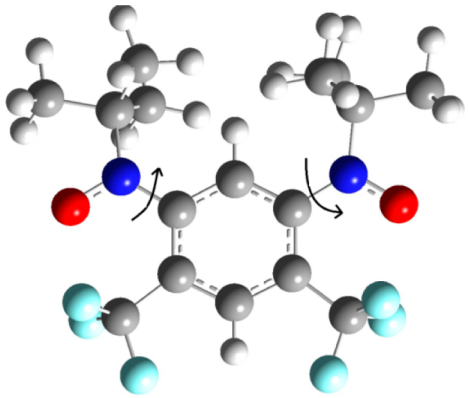

**Figure 1.** The 4,6-trifluoromethyl *m*-phenylene bis(*tert*-butyl)-nitroxide compound (NOFB) for dihedral angles $\theta_1$ and $\theta_2$ (indicated by the two arrows) both fixed to 0°. Atom types are identified by different colors: N (blue), O (red), F(cyan), C (gray), and H (white).

This study confirms that as the molecular conformation changes, the organic diradical switches between ferromagnetic and antiferromagnetic behavior. This property, being of general interest in view of building conformational-based spin switches, has been investigated in detail. In addition, the experimental data available on the NOFB system[33] have been reproduced and interpreted taking also into account thermal effects.

## METHOD AND COMPUTATIONAL DETAILS

The computational route employed here for the study of the spin coupling of diradicals has been widely discussed in our previous articles,[30,31] and it will only be summarized here.

In the framework of post Hartree−Fock methods, it is known that perturbative calculations of *J* have convergence problems due to the neglect of interference effect between excited Slater determinants, not considered in the perturbative computation. On the other hand, for large systems we need to control the dimensions of the variational space which rapidly grows with the molecular dimensions. The most suitable approach, which avoids convergence problems and keeps the variational space at a treatable dimension, is that described as follows (see also refs 30 and 31).

The first step is an SCF calculation of the molecule in its triplet state to obtain a starting set of molecular orbitals (MOs). The second step is a MO localization,[34] where canonical MOs are localized onto specific fragments: in order to retain in the variational calculation, only those pertaining to the fragments involved in the magnetic interaction. Then, a modified set of virtual orbitals (MVOs) is obtained by diagonalizing the Fock operator, modified by the inclusion of additional positive charges on the magnetic sites: as those more effective for the energy gap, we can confidently take as active orbitals for the CI calculation only the lowest MVOs. Finally, accurate *J* values are obtained by a balanced combination of variational and perturbative calculations within the DDCI selection of the configurational space. This final step, named the Complementary Active Space Approach (CSPA), has been already calibrated,[30,31] and a robust protocol for the variational/perturbative balancing has been set up. The DDCI space contains the minimal 4-configuration CAS (2,2) associated with the two magnetic orbitals, one on each NO, all determinants arising from single and double excitation from the magnetic to the virtual orbitals, and double excitations from the magnetic and core orbitals to the virtual orbitals, but involving one single core-to-virtual excitation (see also Figure 3 of ref 18 or Table 1 of ref 31).

For the discussion of the results in the next section, it may be useful to recall the results arising from the "zero order" theory capable of describing symmetric systems characterized by two weakly coupled unpaired electrons. If *a* and *b* are the localized half filled orbitals, the minimal CAS(2,2) space is formed by four Slater determinants

$$|\Psi_A\rangle = |\text{core } a\bar{b}\rangle \tag{1}$$

$$|\Psi_B\rangle = |\text{core } \bar{a}b\rangle \tag{2}$$

$$|\Psi_C\rangle = |\text{core } a\bar{a}\rangle \tag{3}$$

$$|\Psi_D\rangle = |\text{core } b\bar{b}\rangle \tag{4}$$

The first two are the basic Slater determinants which give the largest contributions to the lowest singlet and triplet states, whereas $|\Psi_C\rangle$ and $|\Psi_D\rangle$ are the closed shell charge transfer determinants which only give small contributions to the singlet state. The eigensolutions of this 4 × 4 matrix are easily obtained by treating $\Psi_C$ and $\Psi_D$ within perturbative theory ($U \gg t$). For a system with equivalent magnetic moieties, the singlet triplet energy gap is given by[35]

$$\Delta E_{ST} = 2K_{ab} - \frac{4t_{ab}^2}{U} \tag{5}$$

where $K_{ab} = \langle ab|ba\rangle$ (exchange integral), $t_{ab} = \langle ab|aa\rangle = \langle ab|bb\rangle$ (kinetic exchange), and $U = \langle\Psi_C|H|\Psi_C\rangle - \langle\Psi_A|H|\Psi_A\rangle$, which is usually a large positive number. The two terms of eq 5 always have a different sign and correspond to the ferromagnetic and antiferromagnetic parts, respectively. Further details can be found in the paper by Calzado et al.[18]

The molecular structures have been optimized in the triplet state at the DFT-B3LYP/6-31G* level of theory using the Gaussian package.[36] Unless otherwise stated, all torsional potential energy surfaces have been computed by optimizing all geometries with no symmetry restrictions except the torsional angles investigated.

The canonical molecular orbitals were obtained by a ROHF calculation for the triplet state, using the GAMESS code[37] with the same basis set employed in geometry optimizations. The MVOs were obtained using the Fortran program QUIOLA coded by the authors, which interfaces the GAMESS output files with the routine for the transformation of the integrals from the atomic to the molecular basis set. In each post Hartree−Fock calculation, 1s orbitals of the heavy atoms have always been cut out from the configurational space. All the CI +CSPA calculations have been carried out with the BALOO program written by the authors.


dx.doi.org/10.1021/ct400020x | J. Chem. Theory Comput. 2013, 9, 1958−1963

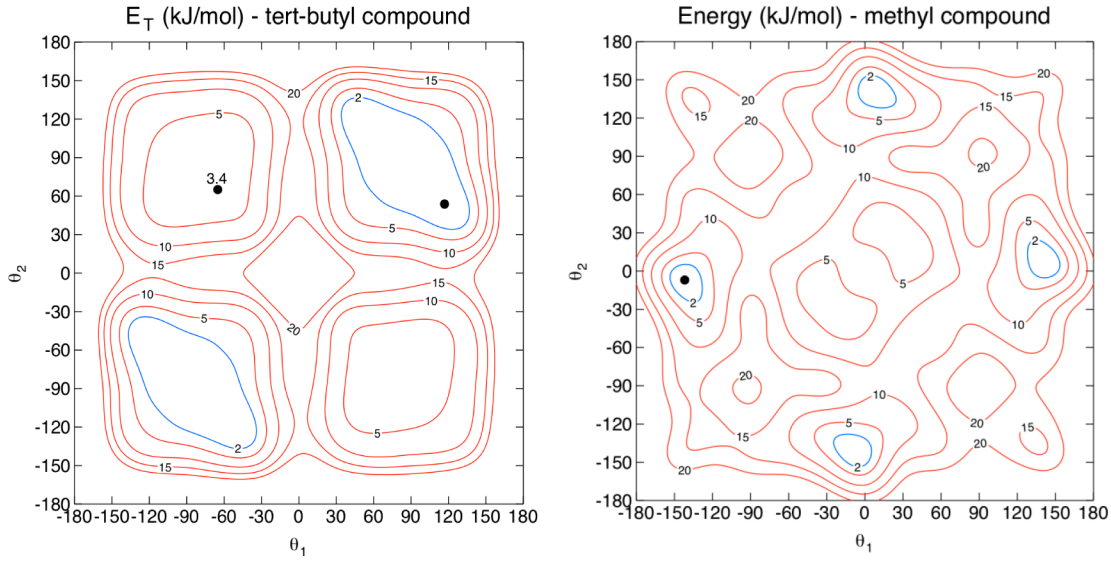


**Figure 2.** Torsional energy of the 4,6-trifluoromethyl *m*-phenylene bis(*tert*-butyl)-nitroxide compound in the triplet state (left) vs dihedral angles $\theta_1$ and $\theta_2$. In the right panel, the same quantity for the model compound with methyl groups in place of the *tert*-butyls. The black dots indicate one of the two equivalent local and absolute minimum energy points with the corresponding energy value. The regions with energy = 2 kJ/mol are marked by blue lines.

## RESULTS AND DISCUSSION

The 4,6-trifluoromethyl *m*-phenylene bis(tert-butyl)-nitroxide (NOFB) is a diradical system with unpaired electrons localized on two magnetic orbitals corresponding to the antibonding orbitals of the N−O groups. The compound is displayed in Figure 1 with the torsional angles $\theta_1$ and $\theta_2$ indicated by arrows. $\theta_1$ and $\theta_2$ are defined in such a way that when both are positive (or negative), the oxygen atoms are on the opposite side with respect to the phenyl ring. The zero value corresponds to the oxygen atoms, coplanar with the bridging ring, pointing toward the closest trifluoromethyl group. From symmetry considerations, the following symmetry relations hold

$$E(\varphi_1, \varphi_2) = E(-\varphi_1, -\varphi_2) = E(\varphi_2, \varphi_1) = E(-\varphi_2, -\varphi_1) \quad (6)$$

Figure 2 (left panel) shows the conformational energy of NOFB in its triplet state vs the torsional angles $\theta_1$ and $\theta_2$. The PES was evaluated by performing calculations at steps of 30° for $\theta_1$ [0°÷180°], $\theta_2$ [−180°÷180°] and optimizing all the remaining internal coordinates; the full PES was then reconstructed using the symmetry relations.

Because of the steric hindrance of the substituents, the structure of the minimum geometry is nonplanar as concerns the NO−phenyl−NO moiety. The PES is dominated by the repulsion between the *tert*-butyl and trifluoromethyl groups, which causes high distortions in the phenyl ring for one or both angles approaching 0° or 180°. The PES shows four well-defined minima corresponding to the nitroxy groups on the same and on the opposite sides of the ring. The opposite side conformation is preferred with an energy difference between the local minimum near −60°,60° and the absolute minimum at 55°,115° (black dots in Figure 2) of 3.4 kJ/mol. From crystallographic data,[33] the two angles are 49° and −70°; i.e., the NO groups are found on the same side with respect to the aromatic ring. This conformation is close to that corresponding to the local minimum at 3.4 kJ/mol (see Figure 2).

Due to the large number of DDCI calculations needed to explore the full PES of the NOFB compound, a smaller model compound (hereafter called NOFM) was obtained, by substituting[38] the methyl groups of the *tert*-butyl moieties with hydrogen atoms. The torsional energy of NOFM is displayed in the right panel of Figure 2, where the very different PES between NOFB and NOFM is apparent. Due to the removal of a large part of the steric repulsion, the PES of NOFM is much more flat with the absolute minimum at 0°,−150°. NOFB was first optimized under the constraint of fixed values of $\theta_1$ and $\theta_2$. Then, $CH_3$ groups were substituted to the *tert*-butyl ones, and finally their geometry was optimized with the constraint that all remaining atoms were fixed in their original position. As discussed in a previous paper,[30] it was accurately verified that this procedure does not significantly alter the value of $\Delta E_{ST}$, while it allows for obvious benefits in terms of computational time.

Experimental evidence indicate that the ground state of NOFB is a triplet with an estimated value of $\Delta E_{ST}$ of ∼55 $cm^{-1}$ at 80 K.[33] It is well-known that this singlet−triplet gap in aromatic bridged nitroxides is highly correlated with the torsional dihedrals $\theta_1$ and $\theta_2$.[2,33,38−40] Moreover, these distortions from planarity in meta substituted aromatic bridges decrease the capabilities of the central ring to act as a ferromagnetic bridge and destabilize the lowest triplet state. In fact, antiferromagnetic behavior (singlet ground state) has been observed[2] in some cases.

The energy splitting surface, computed by using the DDCI +CSPA protocol, is displayed in Figure 3. In the whole $\theta_1$, $\theta_2$ domain, $\Delta E_{ST}$ takes both positive (ferro) and negative (antiferro) values, so that the magnetic behavior depends on the torsional energy profile of the NOFB system. It is apparent that the triplet is the most stable state when both angles are around −180°, 0° or 180° (planar conformations), whereas when one or both angles is near 90°, the singlet state is the ground state. This evidence confirms that when conjugation of the NO−bridge−NO skeleton is not effective, the antiferromagnetic behavior is preferred. In fact, looking at the corresponding compound with hydrogen atoms in place of the $CF_3$ group of ref 30, this has a much higher energy splitting

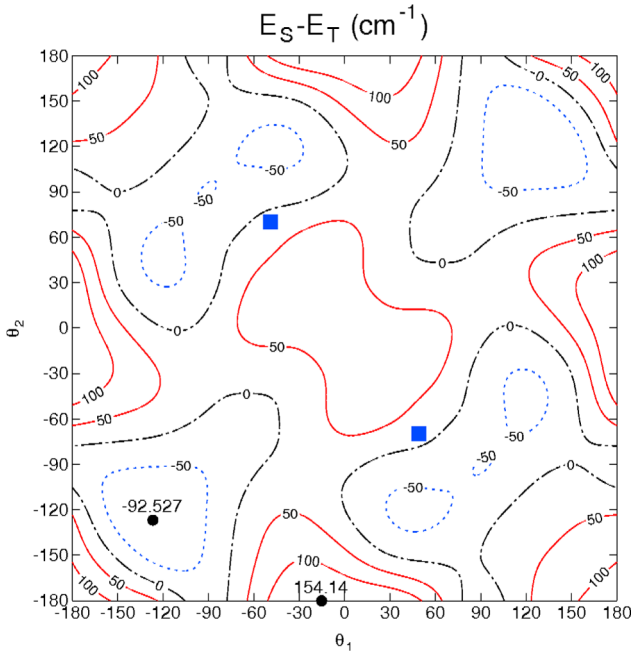


**Figure 3.** Contour plot of the energy splitting $\Delta E_{ST}$ ($cm^{-1}$) of the NOFM compound vs dihedral angles $\theta_1$ and $\theta_2$. The singlet−triplet degeneracy is identified by the black lines. The red and blue lines indicate ferromagnetic and antiferromagnetic regions, respectively. The blue squares indicate the value of the two angles as determined by solid state X-ray spectroscopy.[33] Black dots indicate computed maximum and minimum $\Delta E_{ST}$ values.

(>500 $cm^{-1}$), and we can then deduce that the fluorine has the effect of decreasing the capability of the phenyl bridge to act as a ferromagnetic coupler. The value of the energy splitting at the experimental geometry (blue squares in Figure 3) is slightly negative and close to the zero splitting line and does not allow for drawing any sound conclusion.

A deeper analysis may be done with the data reported in Table 1, referring to few selected conformations. The sign of

**Table 1. Some Relevant Quantities Determining the Singlet Triplet Energy Gap**[a]

| | 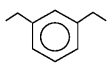 |  | 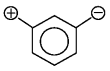 | 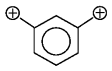 |
|---|---|---|---|---|
| $\theta_1$ $\theta_2$ | 0 0 | 180 180 | 90 90 | 90 -90 |
| $\Delta E_{ST}$ DDCI | +38 | +68 | -45 | -50 |
| $\Delta E_{ST}$ Eq. 5 | +37 | +69 | -11 | -12 |
| $K_{ab}$ | 47 | 39 | 5 | 5 |
| $t_{ab}$ | 1271 | 486 | 770 | 798 |
| $U$ | 113730 | 104785 | 115604 | 115276 |
| NO component | 0.943 | 0.943 | 0.972 | 0.972 |

[a]The last row is the component of the magnetic orbitals on the NO moieties, as determined by Mulliken population analysis. All energies are in $cm^{-1}$ and angles in degrees.

$\Delta E_{ST}$ computed by DDCI calculations and by the simpler perturbative treatment of CAS(2,2) space is the same, suggesting that the latter method includes the essential physics governing the magnetic behavior. It is apparent that the decisive quantity is the $K_{ab}$ exchange integral, which strongly decreases for nonplanar conformations. The $t_{ab}$ integral undergoes relevant changes for all four conformations considered, whereas $U$ shows a minor sensitivity. In the (0°, 0°) ferromagnetic conformation, the coupling between the magnetic centers is maximized as the values of $K_{ab}$, $t_{ab}$, and $U$ take their maximum value. The strong decrease of $t_{ab}$ in going from the (0°, 0°) to the (180°, 180°) conformation is decisive in order to get the highest value of $\Delta E_{ST}$ for the latter. In both ferromagnetic conformations, the approximate value of the energy splitting and the DDCI splitting are almost coincident. Conversely, in the cases of antiferromagnetic interaction (last two columns of Table 1), the values of $\Delta E_{ST}$ obtained by eq 5 differ from those by DDCI, probably for the high contribution of the CT configurations (eqs 3 and 4), which has been demonstrated to be underestimated in the CAS (2,2) approach.[41] The last row reports the component of the magnetic orbitals on the NO moieties, as determined by Mulliken population analysis. The correlation with $K_{ab}$ is evident, as a higher localization on NO corresponds to a lower delocalization on the aromatic ring and, consequently, to a lower overlap between the magnetic orbitals and to a smaller $K_{ab}$. In other words, the property of the central ring to act as a ferromagnetic coupler is strongly correlated with its contribution to the charge density of the magnetic orbitals.

From the torsional energy of the triplet state (left panel of Figure 2) and from the energy gap (Figure 3), the torsional energy of the singlet state can be easily computed. Its contour plot is reported in Figure 4. The energy curves are referred to

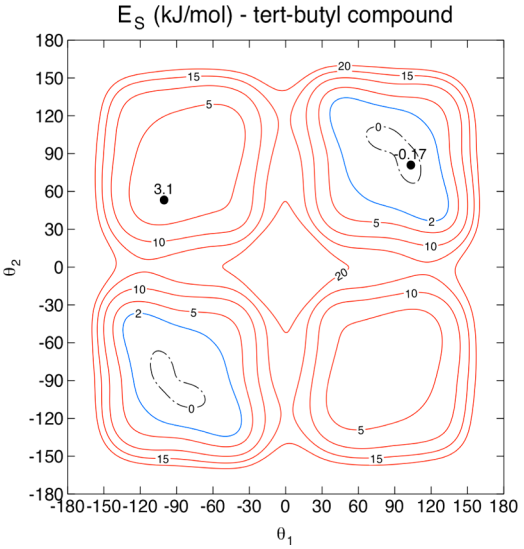


**Figure 4.** Torsional energy of the 4,6-trifluoromethyl *m*-phenylene bis(*tert*-butyl)-nitroxide compound in the singlet state vs dihedral angles $\theta_1$ and $\theta_2$. The black dots indicate the minimum energy points (only one of the four equivalent points is marked) with the energy value. The regions with an energy of 2 kJ/mol are marked by blue lines. The energy is referred to the minimum energy of the triplet state as displayed in Figure 2.

the minimum energy of the triplet state, and they are thus directly comparable with the contour plot of the triplet state. The PES of the singlet state is determined in the hypothesis that once $\theta_1$ and $\theta_2$ are fixed, the geometrical arrangements of the singlet and triplet states are very similar.

The gross features of the singlet PES are the same of the triplet, showing four distinct basins centered at $\theta_1 \pm 90°$ and $\theta_2 = \pm 90°$. Nevertheless, the singlet minimum is slightly displaced with respect to the triplet one, and some regions with negative energy occur. This means that the conformational minimum of


dx.doi.org/10.1021/ct400020x | J. Chem. Theory Comput. 2013, 9, 1958−1963

the singlet state is slightly lower in energy than that of the triplet state. This feature reflects in the temperature dependence of the statistical mean value of the spin given by

$$\langle S^2 \rangle = \frac{\int_{-\pi}^{\pi} d\theta_1 \int_{0}^{\pi} d\theta_2 \, 2 \cdot 3e^{-E_T/kT}}{\int_{-\pi}^{\pi} d\theta_1 \int_{0}^{\pi} d\theta_2 (e^{-E_S/kT} + 3e^{-E_T/kT})} \quad (7)$$

The curve of $\langle S^2 \rangle$ for very low temperatures is reported in Figure 5. The three curves are obtained with different integration ranges of $\theta_1$ and $\theta_2$ in the above equation. Namely, they refer to the absolute minimum basin, the local minimum basin, and the whole range for both angles. By comparing the red and green curves, it is apparent that in this range of temperatures the absolute minimum basin is by far the most populated. The curve referred to the local minimum basin shows a singlet−triplet energy gap more favorable to the singlet (see also Figure 3 around the $\theta_1$ = 90, $\theta_2$ = −90 point). However, the present data show that at very low temperatures the system is antiferromagnetic, and the entropic advantage of the triplet state (degeneracy = 3) prevails on the singlet state for increasing temperature, yielding an asymptotic value of 1.5, consistent with quasi-degenerate singlet and triplet states. Clearly, the data of Figure 5 refer to rather accurate calculations in the gas phase without taking into account possible geometrical distortion due to the packing effect in the solid state. Therefore, these results should be applied with caution when compared with experimental measurements at low temperatures, but we think they can be useful in rationalizing some experimental findings discussed in the following.

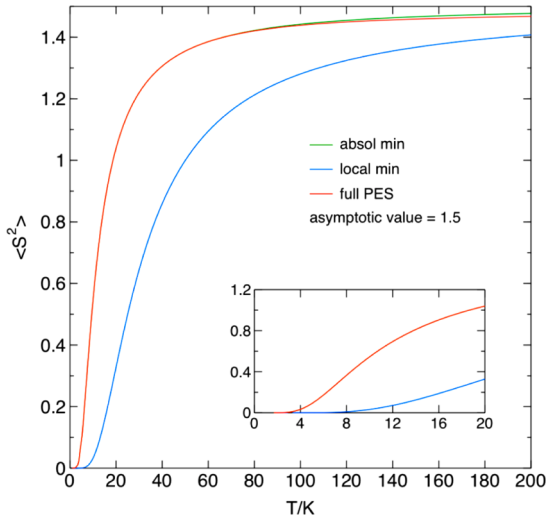


**Figure 5.** Mean statistical value of the spin (in $\hbar^2$ units) of NOFB vs temperature. The three curves are obtained with different integration ranges in eq 7. The green curve refers to to the absolute minimum basin ($\theta_1$ 0°÷180°, $\theta_2$ 0°÷180°), the blue curve to the local minimum basin ($\theta_1$ −180°÷0°, $\theta_2$ 0°÷180°), and the red curve to the whole range for both angles.

In the experiment reported by Rajca et al.,[33] a solution of the present molecule in 2-methyltetrahydrofuran (2-MeTHF) is cooled at 5 K, and after some time a net increase of magnetization up to a value consistent with a triplet was observed. This behavior was not observed for other solvents. The authors hypothesized the existence of two conformers having, respectively, antiferromagnetic and ferromagnetic properties. The antiferromagnetic species is more stable at high temperatures, due probably to environmental effects. Operating a rapid cooling from ambient temperature to 5 K, the frozen high temperature conformer gave small magnetic susceptibility, which was observed to increase in time, up to the value expected for a triplet state.

Our results indeed predict two conformers, both for the triplet and singlet states, corresponding to the two minima of Figure 2 (left) and Figure 4, respectively. The minima differ by about 3 kJ/mol, and the barrier for their interconversion is at least 20 kJ/mol. The energy gap between the two spin states is rather low in both minima, making the magnetic behavior sensitive to entropic effects driven by the temperature. However, in contrast with the hypothesis of Rajca et al.,[33] the singlet state is always the most stable for both conformers, at least in our calculations in the gas phase. Moreover, by looking at Figure 4, the stability of the singlet state seems to be even higher in the local minimum (blue curve vs green curve). Due the small values of $\Delta E_{ST}$ around the minima, we can speculate that the medium effects can strongly affect the magnetic behavior of the molecule in glass solution at very low temperatures, and in particular its effects may be different for the two conformers. In conclusion, our results provide information on the presence of two quasi-degenerate conformers and on the singlet−triplet energy gap, but owing to the neglecting of medium effects, our computations cannot give a definite answer regarding the hypothesis by Rajca et al. that the two conformers have different spin ground states.

## CONCLUSIONS

In this paper, some basic relationships between the molecular conformation and the magnetic properties in organic diradicals have been addressed. In particular, we have faced the problem of determining the singlet−triplet energy gap for a diradical system with two soft torsional degrees of freedom. From a computational point of view, this implies a reliable estimate of the magnetic properties exploring the full PES. The large computational effort has been made possible with the new code written by the authors and called BALOO. To the best of our knowledge, this is the first attempt to calculate a J surface at the post-HF level.

The results have confirmed the dependence of the singlet−triplet energy gap from the torsional angles and in particular that the triplet state is the preferred one when the magnetic orbitals are coupled through conjugation induced by the aromatic bridge. The statistical analysis of the PESs indicates that the system is antiferromagnetic at very low temperatures and switch to ferromagnetic for increasing temperatures, reaching the value expected for quasi-degenerate spin states. Owing to the neglecting of the packing effects acting in the solid state, these results have to be considered with caution but can help in the rationalization of some observed phenomena.

As a matter of fact, the possibility of obtaining accurate estimates of the *J* dependence on structural features, connected to large amplitude motions as dihedral torsional displacements, can be exploited to gain a deeper insight into the mechanisms characterizing aromatic bridged diradicals and flank the experimental findings in the design of novel magnetic switches.

## AUTHOR INFORMATION

### Corresponding Author

*E-mail: vincenzo.barone@sns.it.

## Notes

The authors declare no competing financial interest.

## REFERENCES


(1) Rajca, A.; Shiraishi, K.; Rajca, S. *Chem. Commun.* **2009**, 4372.
(2) Shultz, D. A.; Fico, R. M.; Lee, H.; Kampf, J. W.; Kirschbaum, K.; Pinkerton, A. A.; Boyle, P. D. *J. Am. Chem. Soc.* **2003**, *125*, 15426.
(3) See papers in *Chem. Soc. Rev.* **2011**, *40*.
(4) Rajca, A. *Chem. Rev.* **1994**, *94*, 871.
(5) Koivisto, B. D.; Hicks, R. G. *Coord. Chem. Rev.* **2005**, *249*, 2612.
(6) Murata, H.; Miyajima, D.; Nishide, H. *Macromolecules* **2006**, *39*, 6331.
(7) Itoh, T.; Hirai, K.; Tornioka, H. *Bull. Chem. Soc. Jpn.* **2007**, *80*, 138.
(8) Lee, J.; Lee, E.; Kim, S.; Bang, G. S.; Shultz, D. A.; Schmidt, R. D.; Forbes, M. D. E.; Lee, H. *Angew. Chem., Int. Ed.* **2011**, *50*, 4415.
(9) Rajca, A.; Boratyński, P. J.; Olankitwanit, A.; Shiraishi, K.; Pink, M.; Rajca, S. *J. Org. Chem.* **2012**, *77*, 2107.
(10) Noodleman, L. *J. Chem. Phys.* **1981**, *74*, 5737.
(11) Noodleman, L.; Norman, J. G. *J. Chem. Phys.* **1979**, *70*, 4903.
(12) de Loth, P.; Cassoux, P.; Daudey, J. P.; Malrieu, J.-P. *J. Am. Chem. Soc.* **1981**, *103*, 4007.
(13) Miralles, J.; Daudey, J. P.; Caballol, R. *Chem. Phys. Lett.* **1992**, *198*, 555.
(14) Miralles, J.; Castell, O.; Caballol, R.; Malrieu, J.-P. *Chem. Phys.* **1993**, *172*, 33.
(15) Castell, O.; Caballol, R.; Subra, R.; Grand, A. *J. Phys. Chem.* **1995**, *99*, 154.
(16) de Graaf, C.; Sousa, C.; de Moreira, I. P. R.; Illas, F. *J. Phys. Chem. A* **2001**, *105*, 11371.
(17) Angeli, C.; Calzado, C. J.; Cimiraglia, R.; Evangelisti, S.; Guihéry, N.; Leininger, T.; Malrieu, J.-P.; Maynau, D.; Ruitz, J.-V. P.; Sparta, M. *Mol. Phys.* **2003**, *101*, 1389.
(18) Calzado, C. J.; Cabrero, J.; Malrieu, J.-P.; Caballol, R. *J. Chem. Phys.* **2002**, *116*, 2728.
(19) Calzado, C. J.; Cabrero, J.; Malrieu, J.-P.; Caballol, R. *J. Chem. Phys.* **2002**, *116*, 3985.
(20) Cabrero, J.; Ben Amor, N.; de Graaf, C.; Illas, F.; Caballol, R. *J. Phys. Chem. A* **2000**, *104*, 9983.
(21) Neese, F. *J. Chem. Phys.* **2003**, *119*, 9428.
(22) Queralt, N.; Taratiel, D.; de Graaf, C.; Caballol, R.; Cimiraglia, R.; Angeli, C. *J. Comput. Chem.* **2008**, *29*, 994.
(23) Barone, V.; Cacelli, I.; Ferretti, A.; Girlanda, M. *J. Chem. Phys.* **2008**, *128*, 174303.
(24) Barone, V.; Cacelli, I.; Ferretti, A. *J. Chem. Phys.* **2009**, *130*, 94306.
(25) Calzado, C. J.; Angeli, C.; Taratiel, D.; Caballol, R.; Malrieu, J.-P. *J. Chem. Phys.* **2009**, *131*, 044327.
(26) de Graaf, C.; Caballol, R.; Romo, S.; Poblet, J. M. *Theor. Chem. Acc.* **2009**, *123*, 3.
(27) Calzado, C. J.; Angeli, C.; Caballol, R.; Malrieu, J.-P. *Theor. Chem. Acc.* **2010**, *126*, 185.
(28) Monari, A.; Maynau, D.; Malrieu, J.-P. *J. Chem. Phys.* **2010**, *133*, 44106.
(29) Barone, V.; Cacelli, I.; Ferretti, A.; Prampolini, G. *Phys. Chem. Chem. Phys* **2009**, *11*, 3854.
(30) Barone, V.; Cacelli, I.; Ferretti, A.; Monti, S.; Prampolini, G. *J. Chem. Theory Comput.* **2011**, *7*, 699.
(31) Barone, V.; Cacelli, I.; Ferretti, A.; Monti, S.; Prampolini, G. *Phys. Chem. Chem. Phys.* **2011**, *13*, 4709.
(32) Barone, V.; Cacelli, I.; Ferretti, A.; Prampolini, G. *J. Chem. Phys.* **2009**, *131*, 224103.
(33) Rajca, A.; Lu, K.; Rajca, S.; Ross, C. *J. Chem. Commun.* **1999**, 1249.
(34) Pipek, J.; Mezey, P. G. *J. Chem. Phys.* **1989**, *90*, 4916.
(35) Anderson, P. W. *Phys. Rev.* **1950**, *79*, 350.
(36) Frisch, M. J.; Trucks, G. W.; Schlegel, H. B.; Scuseria, G. E.; Robb, G. E.; Cheeseman, J. R.; Scalmani, G.; Barone, V.; Mennucci, B.; Petersson, G.; Nakatsuji, H.; Caricato, M.; Li, X.; Hratchian, H. P.; Izmaylov, A. F.; Bloino, J.; Zheng, G.; Sonnenberg, J. L.; Hada, M.; Ehara, M.; Toyota, K.; Fukuda, R.; Hasegawa, J.; Ishida, M.; Nakajima, T.; Honda, Y.; Kitao, O.; Nakai, H.; Vreven, T.; Montgomery, J. A.; Peralta, J. E.; Ogliaro, F.; Bearpark, M.; Heyd, J. J.; Brothers, E.; Kudin, K. N.; Staroverov, V. N.; Kobayashi, R.; Normand, J.; Raghavachari, K.; Rendell, A.; Burant, J.; Iyengar, S. S.; Tomasi, J.; Cossi, M.; Rega, N.; Millam, J. M.; Klene, M.; Knox, J. E.; Cross, J. B.; Bakken, V.; Adamo, C.; Jaramillo, J.; Gomperts, R.; Stratmann, R. E.; Yazyev, O.; Austin, A. J.; Cammi, R.; Pomelli, C.; Ochterski, J. W.; Martin, R. L.; Morokuma, K.; Zakrzewski, V. G.; Voth, G. A.; Salvador, P.; Dannenberg, J. J.; Dapprich, S.; Parandekar, P. V.; Mayhall, N. J.; Daniels, A. D.; Farkas, O.; Foresman, J. B.; Ortiz, J. V.; Cioslowski, J.; Fo, D. J. *Gauusian 09*, revision C.01; Gaussian Inc.: Wallingford, CT, 2009.
(37) Schmidt, M. W.; Baldridge, K. K.; Boats, J. A.; Elbert, S. T.; Gordon, M. S.; Jensen, J. H.; Koseki, S.; Matsunaga, N.; Nguyen, K. A.; Su, S. J.; Windus, T. L.; Dupuis, M.; Montgomery, J. A. *J. Comput. Chem.* **1993**, *14*, 1347.
(38) Barone, V.; Cacelli, I.; Cimino, P.; Ferretti, A.; Monti, S.; Prampolini, G. *J. Phys. Chem. A* **2009**, *113*, 15150.
(39) Dvolaitzky, M.; Chiarelli, R.; Rassat, A. *Angew. Chem., Int. Ed.* **1992**, *31*, 180.
(40) Ali, M. E.; Roy, A. S.; Datta, S. N. *J. Phys. Chem. A* **2007**, *111*, 5523.
(41) Angeli, C.; Calzado, C. J. *J. Chem. Phys.* **2012**, *137*, 034104.